수의학 석사 학위논문

Role of TSG-6 and HIF1α on the Proliferation and Metastasis of Canine Mammary Tumor Cells

개 유선 종양 세포에서 TSG-6와 HIF1α의 역할

2023년 2월

서울대학교 대학원

수의학과 임상수의학 (수의내과학) 전공

김 태 현

개 유선 종양 세포에서 TSG-6와 HIF1α의 역할

지도 교수 윤 화 영

이 논문을 수의학 석사 학위논문으로 제출함

2022년 11월

서울대학교 대학원

수의학과 임상수의학 (수의내과학) 전공

김 태 현

김태현의 수의학 석사 학위논문을 인준함

2023년 1월

위 원 장 서 경 원 (인)

부위원장 윤 화 영 (인)

위 원 채 준 석 (인)

Abstract

Role of TSG-6 and HIF1α on the Proliferation and Metastasis of Canine Mammary Tumor Cells

Tae-Hyeon Kim

Division of Clinical Veterinary Medicine

(Veterinary Internal Medicine)

Department of Veterinary School

Seoul National University

HIF1α-induced hypoxia is a major characteristic of solid tumors that plays an important role in cancer growth, metastasis, and chronic inflammation. Tumor necrosis factor (TNF) stimulated gene (TSG)-6 is a strong regulator of anti-inflammatory pathways, but its role in cancer cells remains unclear. We hypothesized that hypoxia up-regulates TSG-6, thereby increasing the metastatic and growth potential of cancer cells. Primary and metastatic canine mammary gland tumor (MGT) cell lines (CIPp and CIPm) were transfected with *TSG-6* specific siRNA and treated with cobalt chloride ($CoCl_2$) for 48 h to chemically induce a hypoxia environment. The expression of hypoxia-inducible factor-1-alpha (HIF1α) was evaluated by RT-qPCR and western blot analysis. The metastatic

ability of cancer cells and cell cycle distribution were assessed with extracellular matrix invasion assays and flow cytometry. HIF1α up-regulation, induced by $CoCl_2$, was significantly inhibited in the *TSG-6*-knockdown group in both canine MGT cell lines. The change in the expression levels of HIF1α corresponded to the change of invading cells in the *TSG-6*-knockdown group. *TSG-6*-knockdown in the hypoxia group showed decreased proliferation, associated with G_2/M phase arrest. HIF1α expression in hypoxic condition is regulated by TSG-6 expression in canine MGT. *TSG-6*-knockdown causes down-regulation of HIF1α, thereby reducing the metastatic and proliferative abilities of cancer cells. TSG-6 in canine MGT has a potential as a therapeutic target in anti-cancer therapy.

Keyword : canine mammary gland tumors, cell cycle, HIF1α, metastasis, siRNA, TSG-6

Student Number : 2021-29309

Table of Contents

1. Introduction

Hypoxia, a low oxygen level, is a common feature of tumors associated with proliferation and metastasis (1). Hypoxic areas are created by an imbalance between the oxygen supply and consumption. As tumor tissues proliferate and expand, the oxygen demand exceeds its supply. Moreover, oxygen diffusion is impaired by the increasing distance between cells and vasculature, resulting in an even more hypoxic environment (2).

In response to hypoxia, changes in gene expression affect angiogenesis and metabolism, thereby promoting tumor growth and survival (3). Hypoxia stimulates angiogenesis to alleviate hypoxic conditions, leading to increased, rapid, and chaotic vessel formation. Consequently, the tumor tissue becomes highly hypoxic with excessive, but dysfunctional vasculature (4). In breast cancer, the hypoxic environment is a fundamental driver of progression, and the expression of HIF1 is associated with high mortality and poor prognosis through increased tumor growth, migration, metastasis, and drug resistance (5, 6). Canine MGT has the highest incidence in female dogs and is a major research target due to its poor prognosis and high metastatic rate (7-9). In addition, it has 99% similarity in genome sequencing to human breast cancer (10). Therefore, exploring the factors affecting hypoxia in canine MGT cells is important in translational aspects.

TSG-6, a protein product of tumor necrosis factor-alpha (TNFα)-stimulated gene-6 is constitutively expressed in certain organs and is induced by inflammatory cytokines (11). It performs various functions such as matrix organization, immune regulation, and cell regulation. Especially, TSG-6 is expressed in mesenchymal stem cells and has an important anti-inflammatory activity (12-14). Recently,

certain studies have reported the relationship between cancer and TSG-6. High expression of TSG-6 in gastric and urothelial carcinoma have been reported to be associated with a poor prognosis (15, 16), suggesting an interaction between tumor cells and TSG-6.

Also, one of the hallmarks of cancer tissues is chronic inflammation (17). HIF1α is related with transcription factors such as NF-κB and TNFα, which are key coordinators of tumor-associated inflammatory signaling (18-19). However, little is known on the role of TSG-6 in cancer, and whether it could regulate HIF1α and affect the chronic inflammation pathways. Evaluating the relationship between cancer hypoxia and TSG-6 will provide a better understanding of the microenvironment of solid tumors. In this study, we investigated whether TSG-6 induces HIF1α and increases cancer cell growth and metastasis in canine MGT cells, and whether TSG-6 could be a target for anti-cancer therapy.

2. Materials and Methods

2.1 Cell lines and cultures

CIPp (primary) and CIPm (metastatic), canine malignant MGT cell lines were obtained from the Laboratory of Clinical Pathology, College of Veterinary Medicine, Seoul National University (Seoul, Republic of Korea). Cells were tested for mycoplasma and were found negative. CIPp and CIPm cells were cultured in Roswell Park Memorial Institute medium (RPMI) (WELGENE, Namcheon, Republic of Korea) with 10% fetal bovine serum, 1% penicillin-streptomycin and 1% Kanamycin. Cells were incubated at 37°C in a humidified atmosphere of 5% CO_2. Cell culture medium was replaced every 2-3 days, and subculture was performed at 80-90% confluency.

2.2 Cobalt chloride treatment

Cobalt(II) chloride ($CoCl_2$) (Sigma Aldrich, St. Louis, MO, USA) was used to induce hypoxic condition during cell culture. $CoCl_2$ was diluted to a concentration of 100 mM in Dulbecco's phosphate buffered saline (DPBS) (WELGENE) and stored at -20°C while blocking the light. When $CoCl_2$ was applied to cancer cells, it was diluted into desired concentrations using the culture medium.

2.3 Transfection with small interfering RNA (siRNA)

Before siRNA transfection, CIPp and CIPm cells were cultured in antibiotic-free medium in a 6 well plate (2.5×10^5 cells/well). When 40% confluency was achieved, cells were transfected with *TSG-6* specific siRNA or scrambled siRNA

(Santa Cruz Biotechnology, Dallas, TX, USA; sc-39819 and sc-37007, respectively) for 48 h using Lipofectamine 2000 (Invitrogen, Waltham, MA, USA), according to the manufacturer`s instructions.

2.4 Cell viability assay

Cell viability was assessed according to the manufacturer's protocol using D-Plus™ CCK cell viability assay kit (CCK-3000) (Dong-in Biotech, Seoul, Republic of Korea). To determine the maximum concentration of $CoCl_2$ that does not induce toxicity in cells, CIPp and CIPm cells were seeded into 96 well plates at 1,000 cells/well and incubated for 24 h. Then, cells were treated with $CoCl_2$ at 0, 50, 75, 100, 125 and 150 μM for 24, 48 and 72 h. Following incubation, cells were treated with 10 μl Cell Counting Kit solution (Dong-in Biotech) and incubated at 37℃ for 1 h. After incubation, the optical density (OD) at absorbance 450 nm for each well were assessed in a Microplate reader (BioTek Instruments, Winooski, VT, USA).

2.5 RNA extraction, cDNA synthesis, quantitative real time PCR (RT-qPCR)

Total RNA of CIPp and CIPm cells was extracted using the Easy-BLUE Total RNA Extraction kit (Intron Biotechnology, Gyeonggi-do, Republic of Korea). For each sample, the concentration and purity were measured by a spectrometer (Implen, Westlake Village, CA, USA). cDNA was synthesized using CellScript All-in-One 5X 1st cDNA Strand Synthesis Master Mix (CellSafe, Seoul, Republic of Korea). For reverse transcription, the reaction mixtures were incubated at 42℃ for 15 min and then reverse transcriptase was inactivated by heat treatment at 85℃ for 5 s. The cDNA samples were assayed in duplicate for RT-qPCR using the

AMPIGENE qPCR Green Mix HI-ROX with SYBR Green Dye (Enzo Life Science, Farmingdale, NY, USA), according to the manufacturer`s instructions. RT-qPCR analysis was performed using the Quantstudio 1 Real-time PCR system (Applied Biosystems, Waltham, MA, USA). The reactions were performed at 50℃ for 2 min then at 95℃ for 10 min, followed by 40 cycles of 95℃ for 30 s and 60℃ for 1 min. mRNA expression levels were normalized to that of glyceraldehyde-3-phosphate dehydrogenase (GAPDH), using the $2^{-\Delta\Delta^{CT}}$ method (20). The primer sequences used are listed in Table I.

2.6 Protein extraction and western blot

Total protein was extracted from cultured cells using the PRO-PREP protein extraction solution (Intron Biotechnology, Seongnam, Republic of Korea). Protein concentration was quantified using the DC protein assay kit (Bio-Rad, Hercules, CA, USA). For the western blot assay, 15 μg of protein were separated by SDS-PAGE gel electrophoresis. After electrophoresis, proteins were transferred to polyvinylidene difluoride membranes (EMD Millipore, Billerica, MA, USA) and then blocked with 5% skim milk in Tris-buffered saline. Membranes were incubated with primary antibodies against HIF1α (1:500; LifeSpan BioSciences, Seattle, WA, USA), TSG-6 (1:500; Santa Cruz Biotechnology), cyclooxygenase (COX)-2 (1:500; Santa Cruz Biotechnology), nuclear factor kappa light chain enhancer of activated B-cells (NF-κB) (1:1000; Cell Signaling Technology, Danvers, MA, USA) and β-actin (1:1,000, Santa Cruz Biotechnology) at 4℃ overnight. Then, a secondary antibody was applied for 2 h at room temperature, and the bands were detected by using chemiluminescence (Advansta, Menlo Park, CA, USA).

2.7 Invasion assay

CIPp and CIPm cells transfected with siRNA were cultured with normal media or 50 μM $CoCl_2$ media for 48 h. CIPp cells were resuspended with serum-free RPMI at a concentration 2×10^6 cells/ml and CIPm was resuspended with serum-free RPMI at a concentration 5×10^5 cells/ml. Eight μm pore transwell membrane (SPL Life Science, Gyeonggi-do, Republic of Korea) was coated with 0.125 M Matrigel (Corning Life Science, Glendale, AZ, USA) and incubated at 37℃ for 30 min. Following this step, 2 ml of complete medium were added to the bottom chamber and 1 ml of serum-free cell suspension medium was added to the upper chamber. Then cells were incubated at 37℃ with 5% CO_2 for 72 h. The upper chamber with cells that did not invade was removed with a cotton swab, and the invaded cells at the lower chamber were fixed with 3.7% formaldehyde, permeabilized with 100% methanol and stained with Giemsa. Cells were counted in a 100X field of view under a light microscope.

2.8 Cell cycle assay

CIPp cells transfected with siRNA were seeded in 6 well plates at a density of 2.5×10^5 cells/well and treated with $CoCl_2$ (0 μM or 50 μM) for 48 h. After harvesting cells for flow cytometry, 1×10^6 cells were prepared per group, fixed with 80% acetone, and washed with DPBS. The cells were stained with 500 μl of propidium iodide/RNase buffer (BD Biosciences, Franklin Lakes, NJ, USA) for 20 min at room temperature in the dark. Cell fluorescence was analyzed by a flow cytometer (FACS Aria II) (BD Biosciences).

2.9 Statistical analysis

The GraphPad Prism (version 5) software (GraphPad Software, San Diego, CA, USA) was used for statistical analyses. One-way analysis of variance (ANOVA) and Two-way analysis of variance (ANOVA) analysis of variance followed by Bonferroni multiple comparison test. Results are shown as the mean±standard deviation. A p-Value < 0.05 was determined to be statistically significant.

Table I. Primer sequences for RT-qPCR of CIPp and CIPm under hypoxic conditions

Target genes	Primers	Sequences (5' → 3')	References
Canine *GAPDH*	Forward	AACATCATCCCTGCTTCCAC	(42)
	Reverse	GACCACCTGGTCCTCAGTGT	(42)
Canine *TSG-6*	Forward	TCCGTCTTAATAGGAGTGAAAGATG	(43)
	Reverse	AGATTTAAAAATTCGCTTTGGATCT	(43)

3. Results

3.1 Cell viability analysis of mammary gland tumors when using $CoCl_2$

To establish whether TSG-6 regulates HIF1α, it was necessary to determine the appropriate concentration of $CoCl_2$ required to create a chemically induced hypoxic environment. The appropriate concentrations of $CoCl_2$ for the CIPp and CIPm cell lines were determined using the CCK-8 assay (Figure 1). CIPp showed a significant decrease in OD value at 150 μM when applied for 24 h ($p < 0.05$), and at 125 μM when applied for 48 and 72 h ($p < 0.005$ and $p < 0.001$, respectively) (Figure 1A-C). CIPm cells showed a significant decrease at concentrations higher than 75 μM after 48 h ($p < 0.05$) (Figure 1D-F). Therefore, 100 μM for CIPp and 50 μM for CIPm, which are the maximum concentrations that did not affect the viability of cancer cells, were applied in subsequent experiments.

3.2 Expression of TSG-6 in tumor cells under hypoxic conditions

TSG-6 expression in CIPp and CIPm cells was analyzed by RT-qPCR and western blotting to confirm whether *TSG-6*-knockdown occurred even after $CoCl_2$ was applied for 48 h after siRNA transfection. RT-qPCR showed a significant decrease in the expression of *TSG-6* in both CIPp and CIPm after transfection (siTSG-6 groups) when compared to control siRNA transfected groups (scRNA groups) (CIPp, $p < 0.005$; CIPm, $p < 0.05$) (Figure 2A and B). The protein expression levels were also reduced in the siTSG-6 group when compared to scRNA groups (CIPp, *p*

< 0.01; CIPm, $p < 0.05$) (Figure 2C-F).

3.3 Relationship between TSG-6 and HIF1α in tumor cells

Western blotting was used to determine whether TSG-6 regulates HIF1α. HIF1α protein expression levels were determined by investigating a $CoCl_2$-untreated group, and a $CoCl_2$ (50 μM)-treated group (Figure 3). In the treated group, the expression of HIF1α increased in both CIPp and CIPm cell lines. On the other hand, in the siTSG-6 groups, HIF1α expression was significantly lower than that in scRNA groups (CIPp, $p < 0.05$; CIPm, $p < 0.01$).

3.4 Hypoxia increases the metastatic capability of the CIPp and CIPm cell lines but not in the TSG-6-knockdown groups

To examine whether TSG-6 regulates the metastatic potential of cancer cells by regulating the expression of HIF1α, an invasion assay was performed. The number of invading cells markedly increased in the group treated with $CoCl_2$ (Figure 4). When compared within the $CoCl_2$-treated groups, both CIPp and CIPm cells significantly decreased the number of invading cells in the siTSG-6 groups, compared to scRNA groups (CIPp, $p < 0.01$; CIPm, $p < 0.001$).

3.5 Cell cycle features were affected in TSG-6-knockdown CIPp

The CIPp cell line was selected for the cell cycle assay. The cell cycle distribution of CIPp cells after hypoxia and *TSG-6*-knockdown was determined using flow cytometry (Figure 5). Under normoxic conditions, CIPp cells were mostly found in the G_0/G_1 phase (57.3±4.9%), followed by the G_2/M phase (26.8±5.2%) and S phase (14±1.13%). Under normoxic conditions, the differences in cell populations

between groups were not significant. However, under hypoxic conditions, the G_0/G_1 phase of the control group and control siRNA transfection group were 61.8±4.73% and 57.3±5.91%, respectively, and the G_0/G_1 phase of the siTSG-6 transfection group was 49.2±0.99% ($p < 0.001$, $p < 0.005$, respectively). The G_2/M phase of the naïve group and scRNA groups were 23.4%±3.35% and 25.1±6.09%, respectively, and the G_2/M phase of the siTSG-6 group was 34.8±0.64% ($p < 0.001$, $p < 0.005$, respectively). The S phase of the naïve group and scRNA group were 14.23±0.76% and 14.5±1%, respectively, and the S phase of the siTSG-6 group was 15.6±0.44% ($p < 0.05$, ns, respectively). Therefore, cell-cycle arrest was induced in the G_2/M phase of CIPp cells by *TSG-6*-knockdown under hypoxia.

4. Discussion

In this study, we investigated the effect of TSG-6 and HIF1α-induced hypoxia in canine MGT cells, focusing on the proliferative and metastatic potential. We used specifically designed commercial siRNA to induce stable knockdown of *TSG-6*. After determining the optimal $CoCl_2$ concentration to induce hypoxia, we confirmed HIF1α expression in both RNA and protein levels. Hypoxia successfully increased HIF1α expression in primary and metastatic canine MGT cells. In the siTSG-6 group, up-regulation of HIF1α was significantly inhibited. Cells showed decreased metastatic ability and proliferation, making TSG-6 an effective target for reducing cancer growth and metastasis.

A hypoxia incubator or chamber is often used to study cancer cell characteristics in a hypoxic environment, but chemically induced hypoxia is also relevant. The advantages of chemically induced hypoxia are that it is less expensive than using a hypoxia chamber or incubator and is stable enough to maintain the hypoxic state. $CoCl_2$ is mostly used to mimic hypoxic conditions (21), created by inducing HIF1α accumulation by replacing Fe^{2+}, a cofactor required for prolyl hydroxylase domain (PHD) activation, to prevent PHD activation and suppress HIF1α degradation (21, 22). However, a high concentration of $CoCl_2$ in culture media could cause cell damage (23). Thus, we confirmed a proper $CoCl_2$ concentration at which the action of TSG-6 could be analyzed without affecting cell growth, using cell viability assay.

HIF is a transcription factor involved in the regulation of genes expressed in cells to adapt to hypoxic environments (24-26). HIF1α has a well-known mechanism and pathway compared to other HIFα subtypes, and many studies have used HIF1α as a marker for hypoxia. HIF1α is expressed throughout the body and is involved in

a cascade of gene expression events for the adaptation to hypoxic environments (26). When expressed in normoxia, HIF1α is hydroxylated by PHD, tagged by the ubiquitination of the Von Hippel-Lindau tumor suppressor protein, and rapidly degraded by the proteasome. However, under hypoxic conditions, the activity of PHD decreases, and HIF1α cannot be hydroxylated; therefore, HIF1α is not degraded and stabilized, allowing it to bind to HIF1β and transcribe the target gene (27). HIF1α plays a key role in many critical aspects of cancer biology, such as angiogenesis, metastasis, and resistance to therapy (2, 27, 28). In Figure 3, the siTSG-6 group showed decreased HIF1α expression at both the RNA and protein level. This revealed that TSG-6 is a factor inducing HIF1α expression in cancer hypoxia. The potential for this mechanism has already been revealed in several papers showing that TSG-6 induces NF-kB activation in inflammatory conditions (29). In addition, the fact that it is involved in STAT3 and TNF-α signaling in various types of immune cells was verified (30-32). Accordingly, the possibility that TSG-6 secreted by tumor cells also possesses the same mechanism is sufficiently raised.

If hypoxia persists, cancer cells become necrotic in the tumor microenvironment, and inflammatory responses occur (1). Inflamed lesions often become more hypoxic due to increased metabolic demands of the cells, which leads to prolonged inflammation (33). Therefore, targeting tumor hypoxia is considered an effective treatment for solid tumors (34). Among them, HIF1α is also considered as a potential target (35-37). One study showed that *in vivo* metastasis of gastric cancer was considerably reduced by HIF inhibition, whereas *in vitro* HIF-deficient cells were less invasive and adhesive (38). But due to complexity of HIF1 pathway regulation, developing effective anti-HIF1α therapy have been declined so far (39,

40). Our data suggest that TSG-6 could regulate HIF1α expression in hypoxic condition, which is a quite encouraging result.

An association between TSG-6 and cancer has recently been reported. In colorectal cancer, TSG-6 overexpression induces CD44 stabilization and reprogramming into cancer-associated fibroblasts through paracrine activation (41). Since gastric carcinoma and chronic inflammation correlate, and there is also a correlation between TSG-6 and inflammatory diseases, it is suggested that TSG-6 may be associated with a poor prognosis related to inflammation control in cancer tissues (42, 43). Although we did not directly confirm the mechanism by which TSG-6 regulates HIF1α, we would like to confirm the mechanism by which TSG-6 regulates tumor cells through follow-up studies. It is also necessary to analyze the effect of TSG-6 secreted by tumors on the growth and metastasis of breast cancer cells at the *in vivo* level.

In conclusion, our data suggest that tumor cell-derived TSG-6 regulates HIF1α expression in hypoxic condition. *TSG-6*-knockdown canine MGT cells reduced cancer proliferative and metastatic abilities, revealing a therapeutic potential of targeting TSG-6 in anti-cancer therapy.

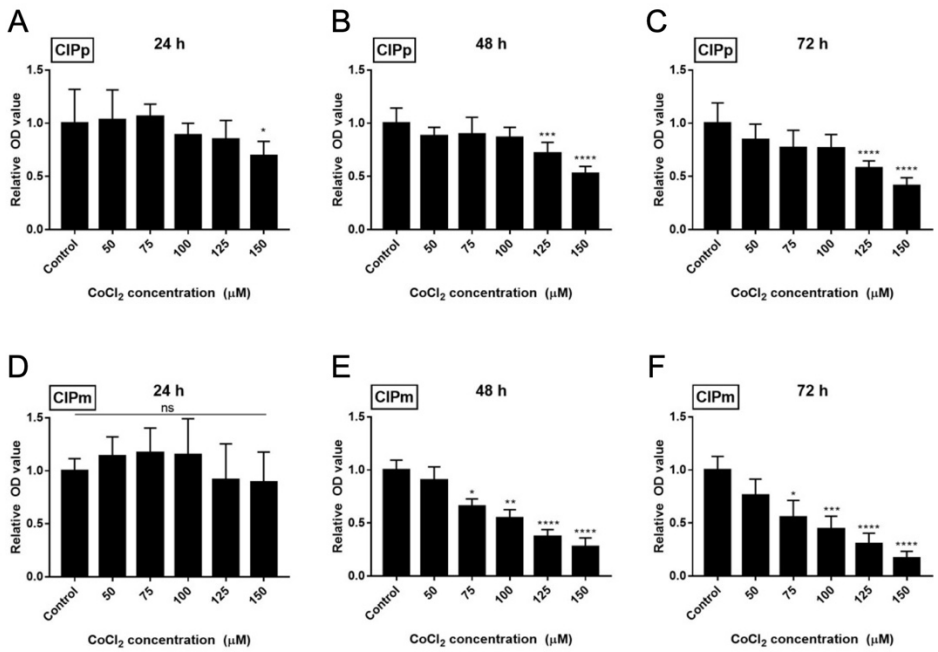

Figure 1. Cell viability assay for cobalt chloride ($CoCl_2$) in CIPp and CIPm. Canine mammary gland tumour cell lines CIPp (A-C) and CIPm (D-F) were treated with various concentration of $CoCl_2$ for 24 h, 48 h and 72 h. Optical density (OD) measurements were obtained at 450 nm absorbance after treatment with 10 µl Cell Counting Kit solution. OD values are presented as the mean±SD of sextuplicate samples, representative of three independent experiments. *$p < 0.05$ *versus* control group, **$p < 0.01$ *versus* control group, ***$p < 0.005$ *versus* control group, ****$p < 0.001$ *versus* control group.

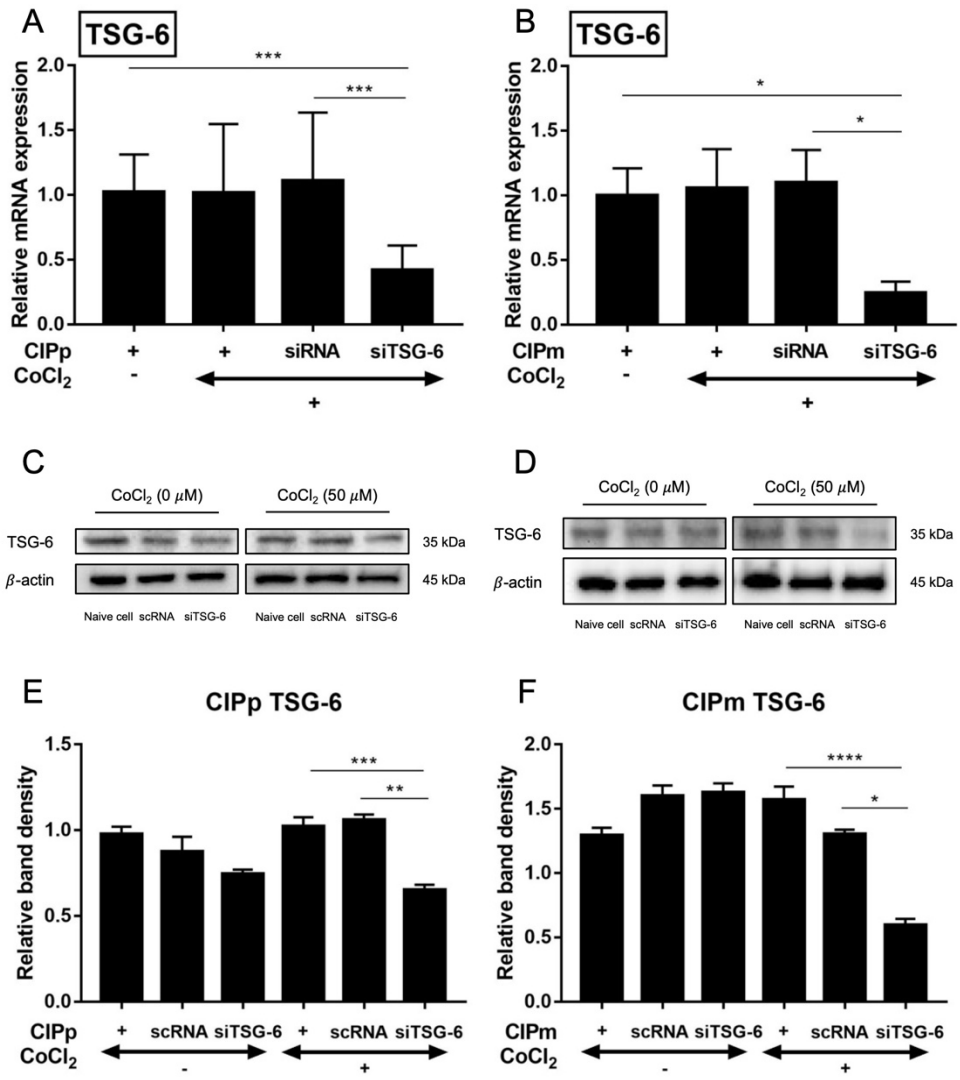
A
TSG-6
Relative mRNA expression
2.0
1.5
1.0
0.5
0.0
***
***
CIPp + + siRNA siTSG-6
CoCl2 - +
B
TSG-6
Relative mRNA expression
2.0
1.5
1.0
0.5
0.0
*
*
CIPm + + siRNA siTSG-6
CoCl2 - +
C
CoCl2 (0 μM)
CoCl2 (50 μM)
TSG-6
β-actin
35 kDa
45 kDa
Naive cell scRNA siTSG-6 Naive cell scRNA siTSG-6
D
CoCl2 (0 μM)
CoCl2 (50 μM)
TSG-6
β-actin
35 kDa
45 kDa
Naive cell scRNA siTSG-6 Naive cell scRNA siTSG-6
E
CIPp TSG-6
Relative band density
1.5
1.0
0.5
0.0
***
**
CIPp + scRNA siTSG-6 + scRNA siTSG-6
CoCl2 - +
F
CIPm TSG-6
Relative band density
2.0
1.5
1.0
0.5
0.0
****
*
CIPm + scRNA siTSG-6 + scRNA siTSG-6
CoCl2 - +

Figure 2. TSG-6 expression in CIPp and CIPm cells with or without cobalt chloride treatment ($CoCl_2$). TSG-6 expression was evaluated by RT-qPCR and western blotting. In RT-qPCR results, RNA expression of TSG-6 in *TSG-6* specific siRNA transfected cells (siTSG-6 group) of both CIPp and CIPm cells was compared to control cells (naïve group) and scrambled siRNA transfected cells (scRNA group) (A, B). Protein TSG-6 expression in the CIPp and CIPm cells was confirmed using western blotting (C, D). Band densities were measured using Image J (E, F). Relative mRNA expression was normalized to that of glyceraldehyde-3-phosphate dehydrogenase (GAPDH), using the $2^{-\Delta\Delta CT}$ method, and presented as the mean±SD of duplicate samples, representative of three independent experiments. *$p < 0.05$ *versus* control group, **$p < 0.01$ *versus* control group, ***$p < 0.005$ *versus* control group, ****$p < 0.001$ *versus* control group.

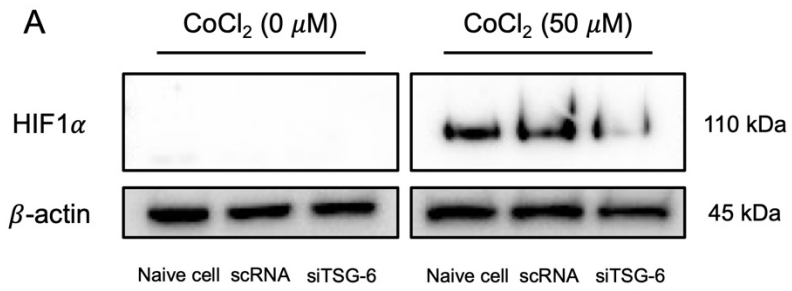
A
CoCl2 (0 μM)
CoCl2 (50 μM)
HIF1α
110 kDa
β-actin
45 kDa
Naive cell scRNA siTSG-6
Naive cell scRNA siTSG-6

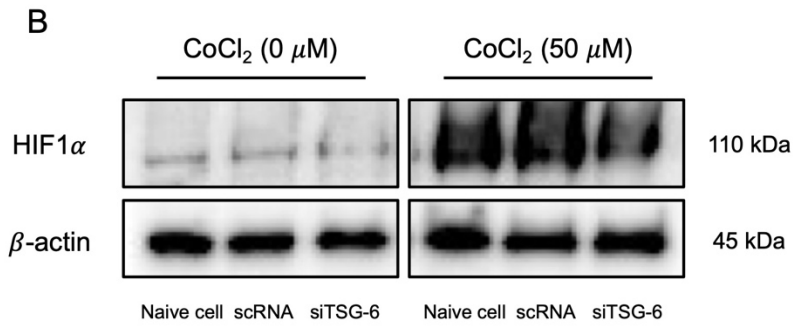
B
CoCl2 (0 μM)
CoCl2 (50 μM)
HIF1α
110 kDa
β-actin
45 kDa
Naive cell scRNA siTSG-6
Naive cell scRNA siTSG-6

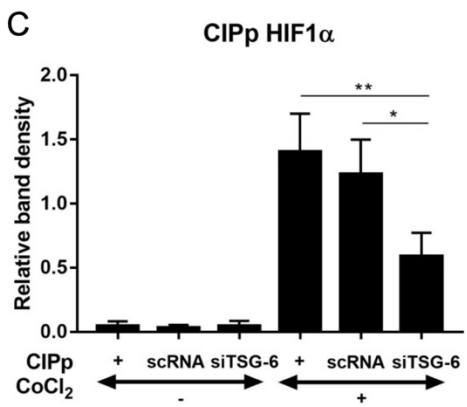
C
ClPp HIF1α
Relative band density
2.0
1.5
1.0
0.5
0.0
**
*
ClPp + scRNA siTSG-6 + scRNA siTSG-6
CoCl2 - +

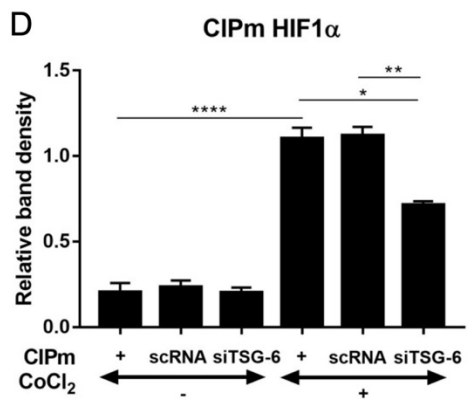
D
ClPm HIF1α
Relative band density
1.5
1.0
0.5
0.0
****
**
*
ClPm + scRNA siTSG-6 + scRNA siTSG-6
CoCl2 - +

Figure 3. Reduction of HIF1α expression in the siTSG-6 group. HIF1α and β-actin (control) protein expression in CIPp (A) and CIPm (B) cells was evaluated by western blotting. Relative band densities are shown for CIPp (C) and CIPm (D). HIF1α band density was estimated using Image J and normalized to that of β-actin. Relative band density was presented as the mean±SD of duplicate samples, representative of three independent experiments. *$p < 0.05$ *versus* control group, **$p < 0.01$ *versus* control group, ***$p < 0.005$ *versus* control group, ****$p < 0.001$ *versus* control group.

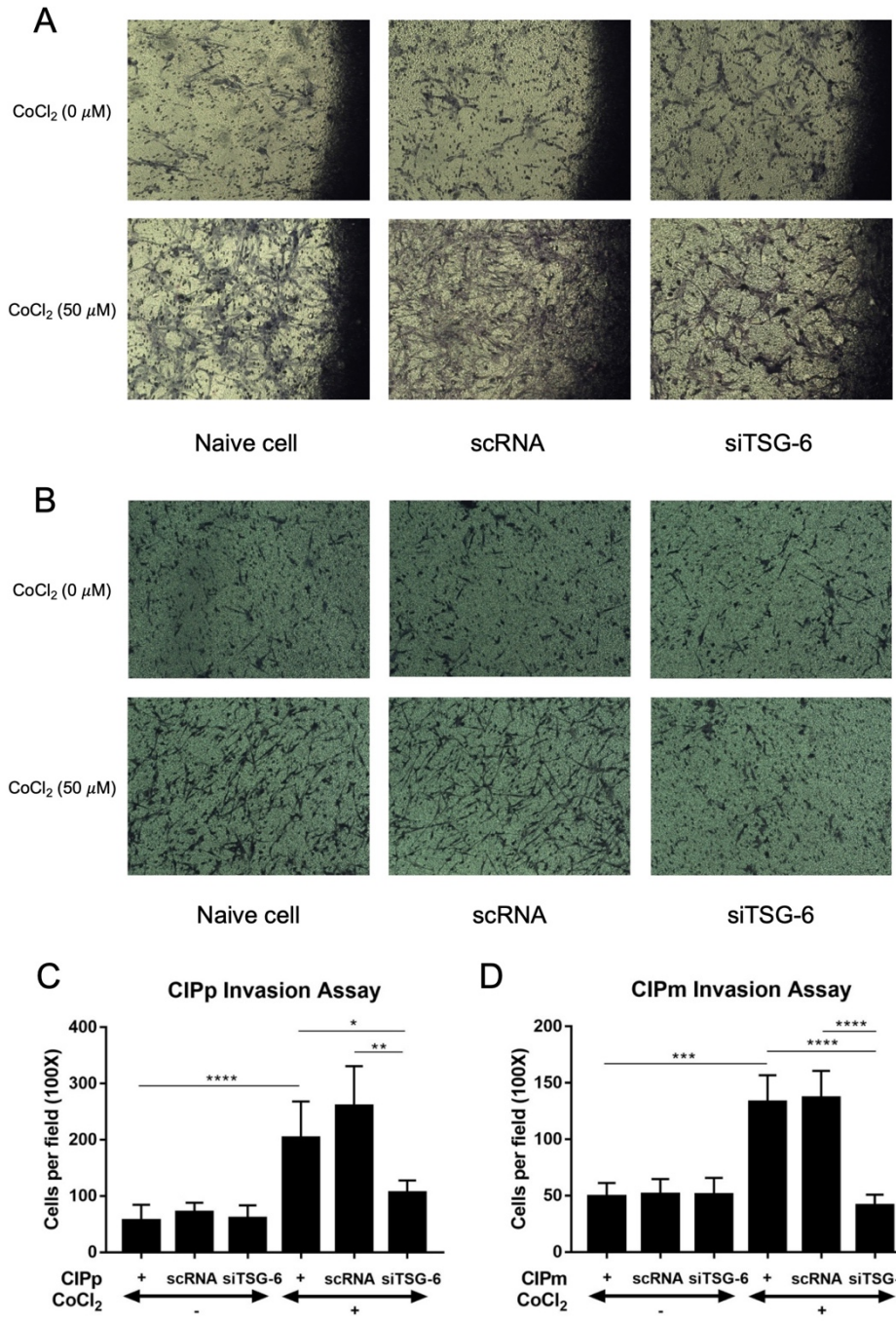
A
CoCl2 (0 μM)
CoCl2 (50 μM)
Naive cell
scRNA
siTSG-6
B
CoCl2 (0 μM)
CoCl2 (50 μM)
Naive cell
scRNA
siTSG-6
C
CIPp Invasion Assay
Cells per field (100X)
400
300
200
100
0
****
*
**
CIPp
CoCl2
+
scRNA
siTSG-6
+
scRNA
siTSG-6
-
+
D
CIPm Invasion Assay
Cells per field (100X)
200
150
100
50
0
***
****
****
CIPm
CoCl2
+
scRNA
siTSG-6
+
scRNA
siTSG-6
-
+

Figure 4. Invasion of CIPp and CIPm cells through an extracellular matrix under cobalt chloride ($CoCl_2$) treatment. The invasive ability of CIPp (A) and CIPm (B) cells was evaluated with extracellular matrix invasion assay with or without *TSG-6*-knockdown, treated in either normal media or $CoCl_2$ 50 μM media for 72 h. Invading CIPp (C) and CIPm (D) cells were counted in x100 field of microscopic view and at least 9 fields were counted. Invading cell number was presented as the mean±SD of duplicate samples and was representative of three independent experiments. *$p < 0.05$ *versus* control group, **$p < 0.01$ *versus* control group, ***$p < 0.005$ *versus* control group, ****$p < 0.001$ *versus* control group.

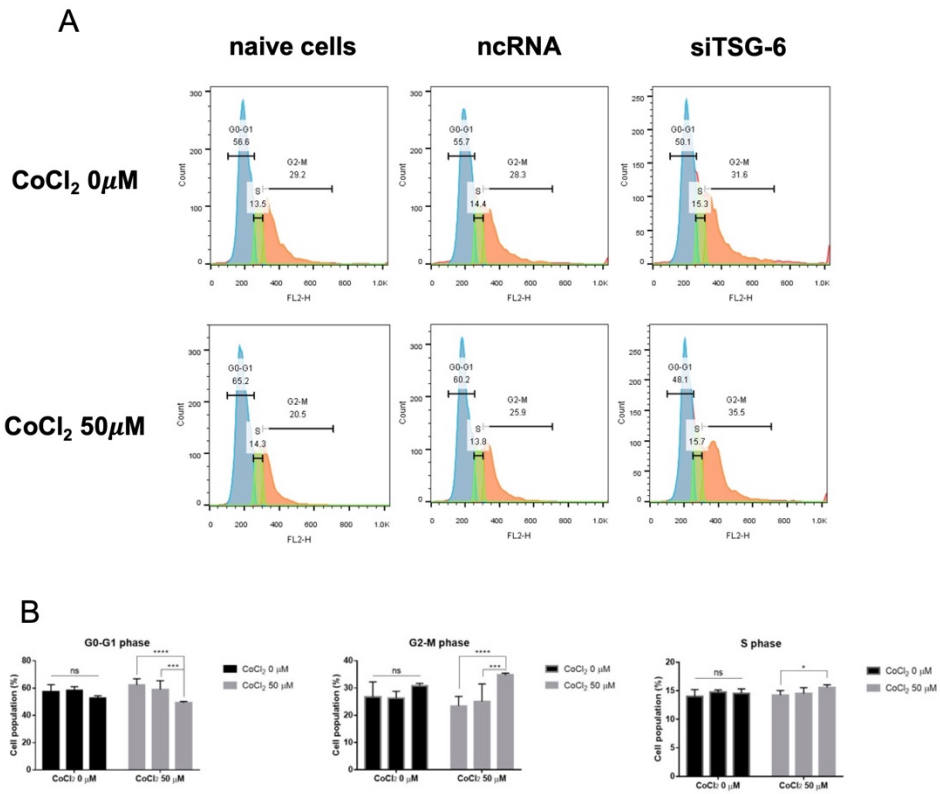

Figure 5. Cell-cycle arrest was induced in the G_2/M phase of CIPp cells by *TSG-6*-knockdown under hypoxic conditions. CIPp cells with or without *TSG-6*-knockdown were treated with either normal media or $CoCl_2$ 50 μM media for 48 h. PI-stained cancer cells were analyzed by flow cytometry for cell cycle distribution analysis (A). The percentages of cells in G_0/G_1, G_2/M, and S phases were compared (B). Data are presented as the mean±SD of duplicate samples, representative of three independent experiments. *$p < 0.05$ *versus* control group, **$p < 0.01$ *versus* control group, ***$p < 0.005$ *versus* control group, ****$p < 0.001$ *versus* control group.

5. References

1. Muz B, de la Puente P, Azab F and Azab AK: The role of hypoxia in cancer progression, angiogenesis, metastasis, and resistance to therapy. Hypoxia (Auckl) *3*: 83-92, 2015.
2. Semenza GL: Hypoxia, clonal selection, and the role of HIF-1 in tumor progression. Crit Rev Biochem Mol Biol *35(2)*: 71-103, 2000.
3. D'Ignazio L, Batie M and Rocha S: Hypoxia and inflammation in cancer, focus on HIF and NF-κB. Biomedicines *5(2):21*, 2017.
4. Carmeliet P and Jain RK: Molecular mechanisms and clinical applications of angiogenesis. Nature *473(7347)*: 298-307, 2011.
5. Wicks EE and Semenza GL: Hypoxia-inducible factors: cancer progression and clinical translation. J Clin Invest *132(11*): e159839, 2022.
6. Courtney EM, Chandra C, Neville JB, and Rodney FM: Hypoxia-mediated drug resistance in breast cancers. Cancer Lett *502*: 189-199, 2021.
7. Salas Y, Marquez A, Diaz D and Romero L: Epidemiological study of mammary tumors in female dogs diagnosed during the period 2002-2012: A growing animal health problem. PLoS One *10(5)*: e0127381, 2015.
8. Moe L: Population-based incidence of mammary tumours in some dog breeds. J Reprod Fertil Suppl *57*: 439-443, 2001.
9. Sorenmo K: Canine mammary gland tumors. Vet Clin North Am Small Anim Pract *33(3)*: 573-596, 2003.
10. Gray M, Meehan J, Martínez-Pérez C, Kay C, Turnbull AK, Morrison LR, Pang LY and Argyle D: Naturally-occurring canine mammary tumors as a translational model for human breast cancer. Front Oncol *1*0: 617, 2020.

11. Day AJ and Milner CM: TSG-6: A multifunctional protein with anti-inflammatory and tissue-protective properties. Matrix Biol *78-79*: 60-83, 2019.
12. An JH, Li Q, Ryu MO, Nam AR, Bhang DH, Jung YC, Song WJ and Youn HY: TSG-6 in extracellular vesicles from canine mesenchymal stem/stromal is a major factor in relieving DSS-induced colitis. PLoS One *15(2)*: e0220756, 2020.
13. Song WJ, Li Q, Ryu MO, Ahn JO, Bhang DH, Jung YC and Youn HY: TSG-6 released from intraperitoneally injected canine adipose tissue-derived mesenchymal stem cells ameliorate inflammatory bowel disease by inducing M2 macrophage switch in mice. Stem Cell Res Ther *9(1)*: 91, 2018.
14. Romano B, Elangovan S, Erreni M, Sala E, Petti L, Kunderfranco P, Massimino L, Restelli S, Sinha S, Lucchetti D, Anselmo A, Colombo FS, Stravalaci M, Arena V, D'Alessio S, Ungaro F, Inforzato A, Izzo AA, Sgambato A, Day AJ and Vetrano S: TNF-stimulated gene-6 is a key regulator in switching stemness and biological properties of mesenchymal stem cells. Stem Cells *37(7)*: 973-987, 2019.
15. Zhang X, Xue J, Yang H, Zhou T and Zu G: TNFAIP6 promotes invasion and metastasis of gastric cancer and indicates poor prognosis of patients. Tissue Cell *68*: 101455, 2021.
16. Chan TC, Li CF, Ke HL, Wei YC, Shiue YL, Li CC, Yeh HC, Lee HY, Huang SK, Wu WJ and Li WM: High TNFAIP6 level is associated with poor prognosis of urothelial carcinomas. Urol Oncol *37(4)*: 293 e11-293 e24, 2019.
17. Hanahan D and Weinberg RA: Hallmarks of cancer: The next generation. Cell *144(5)*: 646-674, 2011. PMID: 21376230. DOI: 10.1016/j.cell.2011.02.013
18. Balamurugan K: HIF-1 at the crossroads of hypoxia, inflammation, and cancer.

Int J Cancer *138(5)*: 1058-1066, 2016.

19. Piasecka D, Braun M, Mieszkowska M, Kowalczyk L, Kopczynski J, Kordek R, Sadej R and Romanska HM: Up-regulation of HIF1-alpha via an NF-κB/COX2 pathway confers proliferative dominance of HER2-negative ductal carcinoma in situ cells in response to inflammatory stimuli. Neoplasia *22(11)*: 576-589, 2020.
20. Livak KJ and Schmittgen TD: Analysis of relative gene expression data using real-time quantitative PCR and the 2(-delta delta c(t)) method. Methods *25(4)*: 402-408, 2001.
21. Munoz-Sanchez J and Chanez-Cardenas ME: The use of cobalt chloride as a chemical hypoxia model. J Appl Toxicol *39(4)*: 556-570, 2019.
22. Kaczmarek M, Cachau RE, Topol IA, Kasprzak KS, Ghio A and Salnikow K: Metal ions-stimulated iron oxidation in hydroxylases facilitates stabilization of HIF-1 alpha protein. Toxicol Sci *107(2)*: 394-403, 2009.
23. Chuntao Y, Hongzhong L, Meifen Z, Zhanli Y, Xiuyu W, Fanqin Z,Chuhuai W and Jianqiang F: Oxidative stress mediates chemical hypoxia-induced injury and inflammation by activating NF-κb-COX-2 pathway in HaCaT cells. Mol Cells *31*: 531-538, 2011.
24. Smith TG, Robbins PA and Ratcliffe PJ: The human side of hypoxia-inducible factor. Br J Haematol *141(3)*: 325-334, 2008.
25. Semenza GL: Defining the role of hypoxia-inducible factor 1 in cancer biology and therapeutics. Oncogene *29(5)*: 625-634, 2010.
26. Semenza GL: Hypoxia-inducible factor 1: Master regulator of O_2 homeostasis. Curr Opin Genet Dev *8(5)*: 588-594, 1998.
27. Ke Q and Costa M: Hypoxia-inducible factor-1 (HIF-1). Mol Pharmacol *70(5)*:

1469-1480, 2006.

28. Semenza GL: Hypoxia-inducible factors: Mediators of cancer progression and targets for cancer therapy. Trends Pharmacol Sci *33(4)*: 207-214, 2012.
29. D'Ignazio L and Rocha S: Hypoxia induced NF-κB. Cells *5(1)*, 2016.
30. Wan YM, Wu HM, Li YH, Xu ZY, Yang JH, Liu C, He YF, Wang MJ, Wu XN and Zhang Y: TSG-6 inhibits oxidative stress and induces M2 polarization of hepatic macrophages in mice with alcoholic hepatitis via suppression of STAT3 activation. Front Pharmacol *11*:10, 2020.
31. Hegde M, Daimary UD, Kumar A, Chinnathambi A, Alharbi SA, Shakibaei M and Kunnumakkara AB: STAT3/HIF1A and EMT specific transcription factors regulated genes: Novel predictors of breast cancer metastasis. Gene *818*: 146245, 2022.
32. Bryan C, Sammour I, Guerra K, Sharma M, Dapaah-Siakwan F, Huang J, Zambrano R, Benny M, Wu S, Young K: TNFα-stimulated protein 6 (TSG-6) reduces lung inflammation in an experimental model of bronchopulmonary dysplasia. Pediatr Res *85(3)*: 390-397, 2019.
33. Eltzschig HK and Carmeliet P: Hypoxia and inflammation. N Engl J Med *364(7)*: 656-665, 2011.
34. Jing X, Yang F, Shao C, Wei K, Xie M, Shen H, Shu Y: Role of hypoxia in cancer therapy by regulating the tumor microenvironment. Mol Cancer *18(1)*: 1-15, 2019.
35. Rogalska A, Forma E, Bryś M, Śliwińska A and Marczak A: Hyperglycemia-associated dysregulation of O-GlcNAcylation and HIF1A reduces anticancer action of metformin in ovarian cancer cells (SKOV-3). Int J Mol Sci *19(9)*: 2750, 2018.

36. Wang Y and Minko T: A novel cancer therapy: combined liposomal hypoxia inducible factor 1 alpha antisense oligonucleotides and an anticancer drug. Biochem Pharmacol *68(10)*: 2031-2042, 2004.
37. Shang-you Y, Elka G, Will X and Anyu W: Effects of hypoxia on proliferation and apoptosis of osteosarcoma cells. Anticancer Res *41 (10)*: 4781-4787, 2021.
38. Rohwer N, Lobitz S, Daskalow K, Jöns T, Vieth M, Schlag P M, Kemmner W, Wiedenmann B, Cramer T and Höcker M: HIF-1α determines the metastatic potential of gastric cancer cells. Br J Cancer *100(5)*: 772-781, 2009.
39. Semenza GL: Targeting HIF-1 for cancer therapy. Nat Rev Cancer *3(10)*: 721-732, 2003.
40. Soni S and Padwad YS: HIF-1 in cancer therapy: two decade long story of a transcription factor. Acta Oncol *56(4)*: 503-515, 2017.
41. Liu B, Liu T, Liu Y, Feng X, Jiang X, Long J, Ye S, Chen D, Wang J and Yang Z: TSG-6 promotes cancer cell aggressiveness in a CD44-dependent manner and reprograms normal fibroblasts to create a pro-metastatic microenvironment in colorectal cancer. Int J Biol Sci *18(4)*: 1677-1694, 2022.
42. Hernandez EG, Partida-Rodriguez O, Camorlinga-Ponce M, Nieves-Ramirez M, Ramos-Vega I, Torres J and Perez-Rodriguez M: Genotype B of killer cell immunoglobulin-like receptor is related with gastric cancer lesions. Sci Rep *8(1)*: 6104, 2018.
43. Chen X, Xu C, Hong S, Xia X, Cao Y, McDermott J, Mu Y and Han JJ: Immune cell types and secreted factors contributing to inflammation-to-cancer transition and immune therapy response. Cell Rep *26(7)*: 1965-1977, 2019.
44. Moon HJ, Finney J, Xu L, Moore D, Welch DR and Mure M: MCF-7 cells expressing nuclear associated lysyl oxidase-like 2 (LOXL2) exhibit an

epithelial-to-mesenchymal transition (EMT) phenotype and are highly invasive in vitro: J Biol Chem *288(42)*: 30000-30008, 2013.

45. Yi Z, Stunz LL and Bishop GA: CD40-mediated maintenance of immune homeostasis in the adipose tissue microenvironment. Diabetes *63(8)*: 2751-2760, 2014.

국문 초록

개 유선 종양 세포에서 TSG-6와 HIF1α의 역할

개의 유선 종양은 암컷 개에서 가장 호발하는 고형 종양으로 알려져 있다. 저산소증 유발 인자-1-알파(HIF1α) 에 의한 저산소증은 암 성장, 전이, 만성 염증에 중요한 역할을 하는 고형 종양의 주요 특징이다. 종양 괴사 인자(TNF) 자극 유전자(TSG)-6은 항염증 경로의 강력한 조절자이지만 암세포에서의 역할은 아직 불분명하다. 우리는 저산소증이 TSG-6을 상향 조절하여 암세포의 전이 및 성장 잠재력을 증가시킨다는 가설을 세웠다. 원발성 및 전이성 개 유선 종양 세포주(CIPp 및 CIPm)를 TSG-6 특이적 siRNA로 발현을 약화시키고 염화 코발트($CoCl_2$)로 48시간 동안 처리하여 화학적으로 저산소증 환경을 유도했다. HIF1α의 발현은 RT-qPCR 및 western blot 분석을 통해 평가하였다. 암세포의 전이 능력 및 세포 주기 분포는 세포외 기질 침습 분석 및 유세포 분석으로 평가하였다. $CoCl_2$에 의해 유도된 HIF1α 상향 조절은 두 개의 세포주 (CIPp, CIPm)에서 확인되었으나 TSG-6 발현 약화 그룹에서 유의미하게 억제되었다 (CIPp 51.9% 감소, $p < 0.05$; CIPm 37.6% 감소, $p < 0.01$). HIF1α의 발현 수준의 변화는 TSG-6 발현 약화 그룹에서 침입 세포의 변화에 상응하였다 (CIPp 58.7% 감소, $p < 0.01$; CIPm 69.5% 감소, $p < 0.001$). 저산소증 그룹의 TSG-6 발현 약화는 G2/M 주기 정지와 관련하여 증식이 감소하는 것을 보여주었다. 저산소 상태에서 HIF1α 발현은 개 유선 종양 세포주에서 TSG-6 발현에 의해 조절된다. TSG-6 발현 약화는 HIF1α의 하향 조절을 유발하여 암세포의 전이 및 증식 능력을 감소시킨다. 그러므로 개 유선 종양 세포의 TSG-6은 항암 요법의 치료 표적으로 고려할 수 있는 잠재력이 있다.

주요어 : 개 유선 종양, 세포 주기, HIF1α, 전이, siRNA, TSG-6

학번 : 2021-29309